114–125 *Nucleic Acids Research, 2005, Vol. 33, No. 1*
doi:10.1093/nar/gki155

Translation of stable hepadnaviral mRNA cleavage fragments induced by the action of phosphorothioate-modified antisense oligodeoxynucleotides

Peter Hasselblatt*, Birgit Hockenjos, Christian Thoma, Hubert E. Blum and Wolf-Bernhard Offensperger

Department of Medicine II, University of Freiburg, Hugstetter Strasse 55, D-79106 Freiburg, Germany

Received November 15, 2004; Revised and Accepted December 9, 2004

ABSTRACT

Phosphorothioate-modified antisense oligodeoxynucleotides (ASOs) are used to suppress gene expression by inducing RNase H-mediated cleavage with subsequent degradation of the target mRNA. However, previous observations suggest that ASO/RNase H can also result in the generation of stable mRNA cleavage fragments and expression of truncated proteins. Here, we addressed the underlying translational mechanisms in more detail using hepadnavirus-transfected hepatoma cells as a model system of antisense therapy. Generation of stable mRNA cleavage fragments was restricted to the ASO/RNase H pathway and not observed upon cotransfection of isosequential small interfering RNA or RNase H-incompetent oligonucleotides. Furthermore, direct evidence for translation of mRNA fragments was established by polysome analysis. Polysome-associated RNA contained cleavage fragments devoid of a 5′ cap structure indicating that translation was, at least in part, cap-independent. Further analysis of the uncapped cleavage fragments revealed that their 5′ terminus and initiation codon were only separated by a few nucleotides suggesting a 5′ end-dependent mode of translation, whereas internal initiation could be ruled out. However, the efficiency of translation was moderate compared to uncleaved mRNA and amounted to 13–24% depending on the ASO used. These findings provide a rationale for understanding the translation of mRNA fragments generated by ASO/RNase H mechanistically.

INTRODUCTION

Antisense technologies are widely used to suppress gene expression in the laboratory and in the clinic as a promising therapy of viral and malignant diseases (1–3). Most studies to date have focused on phosphorothioate-modified antisense oligodeoxynucleotides (ASOs) that hybridize to complementary mRNA. The mRNA portion of the resulting heteroduplex is subsequently targeted for endonucleolytic cleavage by the ubiquitously expressed RNase H (4,5). The resulting mRNA cleavage fragments are supposed to be rapidly degraded by cellular exonucleases thereby rendering the message permanently untranslatable.

However, we have reported previously that ASO-induced cleavage of the target mRNA is not always followed by rapid degradation of the cleavage fragments. ASO directed against hepadnaviral mRNA resulted in the generation of stable 3′ mRNA cleavage fragments in human and avian cells (6). The expression of N-terminally truncated proteins matching the primary sequence of the 3′ mRNA cleavage fragments suggested that these mRNA intermediates may serve as a template for translation. Stable mRNA intermediates and translation of truncated protein were not a peculiarity of viral RNA and also observed using ASO directed against mRNA encoding fluorescent proteins and a cellular transcription factor. These findings implicate that the expression of novel polypeptides with unknown biological properties after

*To whom correspondence should be addressed. Tel: +43 1 797 30; Fax: +43 1 798 71 53; Email: Hasselblatt@imp.univie.ac.at
Correspondence may also be addressed to Wolf-Bernhard Offensperger. Tel: +49 781 471 12 22; Fax: +49 781 471 16 02; Email: Offensperger@josefsklinik.de
Present addresses:
Peter Hasselblatt, Research Institute of Molecular Pathology, Dr Bohr-Gasse 7, A-1030 Vienna, Austria
Christian Thoma, EMBL, Gene Expression Program, Meyerhofstrasse 1, D-69117 Heidelberg, Germany
Wolf-Bernhard Offensperger, St Josefsklinik, Weingartenstrasse 70, D-77654 Offenburg, Germany

ASO/RNase H-mediated cleavage of the target mRNA may cause serious side effects of antisense therapy.

Besides ASO/RNase H, RNA interference (RNAi) mediated by small interfering RNA (siRNA) is commonly used to inhibit gene expression by inducing endonucleolytic cleavage of the target mRNA (7). The antisense strand of siRNA guides a nuclease complex RISC (RNA-induced silencing complex) to the complementary target mRNA and induces its cleavage in the center of the 21 nt siRNA/mRNA duplex, similar to RNase H that cleaves 8–12 nt downstream the 5′ mRNA end of the mRNA/ASO heteroduplex (8,9). In addition, RNase H and RISC both produce 3′-hydroxy and 5′-phosphate termini, and recent analysis even revealed a similar crystal structure of the endonucleolytic domains within RISC and RNase H (9–11). These findings raise the question whether stable 3′ mRNA cleavage fragments and the expression of truncated proteins also occur within the RNAi pathway.

The biological relevance of such stable cleavage fragments will be primarily determined by their translational efficiency. Translation of eukaryotic mRNA is a tightly regulated process with initiation being the rate-limiting step. mRNA structures such as the 5′ cap structure (m^7GpppN) and 3′ poly(A) tail act synergistically with several eukaryotic initiation factors (eIF) to recruit the small ribosomal subunit to the mRNA 5′ terminus (12,13). The 5′ cap structure is considered to play an essential role in this process by binding of the heteromultimeric initiation complex eIF4F via its cap binding subunit eIF4E. This preinitiation complex scans along the mRNA until a favorable initiation codon is encountered (14). As RNase H-mediated cleavage produces 5′ phosphate termini, stable 3′ mRNA cleavage fragments are predicted to lack a cap structure as confirmed previously by RNA ligation and RT–PCR (6). Several mechanisms may thus account for the translation of the stable 3′ mRNA cleavage fragments. Initiation of translation may be cap-independent but 5′ end-dependent as observed *in vitro* and, albeit with severely reduced efficiency, *in vivo* (15–17). A fraction of the mRNA 3′ cleavage fragments may also be recapped by an unknown mechanism, thus enabling cap-dependent translation. The lack of a 5′ cap structure could further be bypassed by direct binding of ribosomes to internal RNA secondary structures called internal ribosome entry sites (IRESs) present on various viral and cellular RNAs (18).

Here, we further examined the translation of stable 3′ mRNA cleavage fragments using ASO directed against duck hepatitis B virus (DHBV) in hepatoma cells as a model system of antisense therapy for hepadnaviral infection. Hepatitis B virus (HBV) infection is a major cause of chronic liver disease including liver cirrhosis and hepatocellular carcinoma (19). DHBV and HBV share basic characteristics in viral replication and DHBV infection is therefore a relevant experimental model for the evaluation of new antiviral strategies (20). The DHBV genome consists of a partially double-stranded circular DNA of 3021 bp length. Two major viral transcripts generated by the host cellular polymerase II include the overlapping pregenomic RNA (pgRNA, 2530–3021/1–2796) and long subgenomic RNA (sgRNA 740–2796). pgRNA codes for viral core proteins, the reverse transcriptase/DNA polymerase and serves as a template for reverse transcription during viral replication. The sgRNA encodes the viral surface proteins (preS/S and S). PreS/S proteins are translated by a leaky scanning mechanism using four distinct start codons yielding the preS/S isoforms p36, p35, p33 and p30, respectively (21). Thus, DHBV mRNAs are particularly suitable to study the translation of mRNA cleavage fragments into truncated preS/S protein because several initiation codons yielding distinct protein isoforms are present.

Here, we provide evidence that the generation of stable 3′ mRNA cleavage fragments and expression of truncated proteins is restricted to the ASO/RNase H pathway. We further demonstrate that these mRNA fragments are translated with moderate efficiency and our data suggest that a 5′ end-dependent and, at least in part, cap-independent mechanism is involved.

MATERIALS AND METHODS

Plasmids

DHBV RNAs were expressed from different plasmids: pGemDHBV is a replication-competent head-to-tail dimer construct coding for DHBV F16 (22), pDHBVsg codes only for sgRNA under control of a CMV promoter (6) and HTD-Dcore$^-$ encodes a DHBV mutant deficient of the viral core protein (23). *Renilla* and firefly luciferase were expressed from vectors pRL-TK and pGl2-control (Promega, Mannheim, Germany) and a CMV promoter was inserted into pGl2 to improve the expression in LMH cells. A preS luciferase fusion construct (preS-Luc) was obtained by cloning a DHBV fragment comprising the 5′-untranslated region (5′–UTR) of the subgenomic RNA and preS region (nucleotides 740–1094) in frame into the HindIII site of pGL2 control. The pEGFP encodes enhanced green fluorescent protein (EGFP). A dicistronic vector with EGFP as the first cistron and preS-Luc as the second cistron was constructed by the insertion of a NheI/NotI fragment of pEGFP comprising the open reading frame into the 5′ multiple cloning site of preS-Luc. For *in vitro* transcription, the preS portion of preS-Luc including the T7 promoter was cloned into pT3Luc(pA) encoding a polyadenylated firefly luciferase mRNA (A_{98}) (24).

Antisense oligonucleotides

Phosphorothioate-modified high-performance liquid chromatography (HPLC)-purified 18mer ASO and isosequential 2′-*O*-methyl-modified RNA oligonucleotides were obtained from Microsynth (Balgach, Switzerland): ASO DHBV795, 5′-ATGTTGCCCCATCATAAA-3′; ASO DHBV874, 5′-TTGGGATCATTCTTCCGG-3′; and ASO Luc, 5′-TCGAAGTATTCCGCGTACG-3′. As controls, ASO with unrelated sequences (ASO 54, 5′-CAGTCACTAAGTCACTGG-3′ or ASO 507, 5′-GGAGTCGGCCGACTCCAT-3′) or a mismatch control (ASO DHBV795miss, 5′-ATGTTGTTTAAACATAAA-3′) were used. As no effect on the target mRNA or protein was observed with either control ASO, only one control was included in each experiment. HPLC-purified siRNA consisting of 19mer double-stranded RNA with two 3′ overhanging thymidines were obtained from Xeragon (Zürich, Switzerland). The siRNA DHBV794 was directed against DHBV794-812 (5′-ATTTATGATGGGGCAACAT-3′) corresponding to the target sequence of ASO DHBV794. Single-stranded siRNA (ssRNA794 and asRNA794) and double-stranded siRNA with inverse sequence were used as controls.

Cell culture and transfections

The avian hepatoma cell line LMH supports replication of DHBV (25). Cells were cultured in Isocove's modified Dulbecco's medium (GIBCO-BRL, Karlsruhe, Germany). The medium contained 7% fetal bovine serum (Biochrom, Berlin, Germany), penicillin (100 U/ml), streptomycin (100 μg/ml; both GIBCO-BRL) and 1% of a non-essential amino acid stock solution (GIBCO-BRL). Cells were transfected with DNA using the calcium phosphate method. In a typical cotransfection experiment, 5 μg of plasmid DNA and 5 μg of ASO were used per 10 cm dish. To examine whether the effects of the different antisense compounds were concentration-dependent, cells were seeded in 6-well plates and cotransfected with 1 μg of plasmid DNA and different amounts of antisense compounds (0, 0.1, 0.5, 1 and 2 μg, respectively, corresponding to 0, 7, 33, 67 and 133 pmol of siRNA or 0, 18, 91, 184 and 367 pmol of ASO, respectively). Cells were harvested after 2 days for further analysis.

The Transmessenger kit (Qiagen, Hilden, Germany) was used for RNA transfections according to the manufacturer's instructions. An aliquot of 1 μg of mRNA and 1 μg of ASO were cotransfected per 6-well plate in a typical cotransfection experiment.

RNA analysis

Total cellular RNA was isolated using the Trizol reagent (Invitrogen, Karlsruhe, Germany) or the RNeasy kit (Qiagen). RNA was separated on formaldehyde containing 1.2% agarose gels, blotted onto Nylon membranes (Hybond N; Amersham Pharmacia, Freiburg, Germany) by capillary transfer and visualized using ^{32}P-labeled oligo probes or DNA fragments as indicated.

Total cellular RNA and cytoplasmic RNA were prepared from the same sample to determine the percentage of cytoplasmic RNA. Cells were washed twice with phosphate-buffered saline (PBS) and lyzed (lysis buffer 10 mM Tris, pH 7.5, 10 mM NaCl, 8 mM $MgCl_2$, 1 mM DTT, 1.5 mM PMSF, 1% Triton X-100 and 0.5% sodium desoxycholate). Nuclei and debris were removed by centrifugation at 10 000 r.p.m. for 10 min in a microcentrifuge and cytoplasmic RNA from the supernatant was isolated with Trizol. Total cellular and cytoplasmic RNA were compared by northern-blot analysis using probes that bind to a region 3′ of the putative cleavage site on sgRNA or to EGFP and subsequently quantified using phosphorimaging.

For run-off *in vitro* transcription of capped mRNA, 4 μg of linearized DNA template was incubated with T7 transcription buffer (Promega) containing 8 mM cap analog (m^7GpppG; NEB, Frankfurt, Germany), nucleotide mixture (1 mM of each CTP, ATP and UTP; Promega), RNasin (NEB) and 60 U of T7 RNA polymerase (Promega). After incubation at 37°C for 5 min, 1 mM GTP was added and incubated for 2 h with subsequent DNase I digestion (GIBCO-BRL). RNA was recovered using the RNeasy kit and analyzed by gel electrophoresis.

Polysome analysis

Polysome analysis was performed as described with minor modifications (26). All steps were performed on ice and cells from 2 to 5 10-cm dishes were used per gradient. Cells were washed with ice-cold PBS containing 0.1 mg/ml of cycloheximide and lyzed on the plate with polysome extraction buffer (15 mM Tris–HCl, pH 7.4, 15 mM $MgCl_2$, 0.3 M NaCl, 1% Triton X-100, 0.1 mg/ml of cycloheximide and 1 mg/ml of heparin). Extracts were transferred to Eppendorf tubes and incubated on ice. Nuclei and debris were removed by centrifugation at 10 000 r.p.m. for 10 min in a microcentrifuge. Supernatants were layered onto 10 ml of 10–50% sucrose gradients composed of extraction buffer lacking Triton X-100. The gradients were centrifuged at 35 000 r.p.m. at 4°C using a Kontron TST41.14 rotor for 190 min. After centrifugation, 30 fractions were collected and the absorbance at 254 nm was determined for each fraction using a photometer. Three fractions each were pooled before RNA isolation. $MgCl_2$ was replaced by EDTA in the EDTA release experiment.

RNA ligation and RT–PCR

To analyze the capping status of polysome-associated RNA, cells were cotransfected and cytoplasmic extracts were analyzed by sucrose gradient centrifugation. The gradient was directly fractionated omitting the determination of the absorbance profile in order to minimize mRNA degradation before RNA ligation and RT–PCR. Half of each fraction was further analyzed by northern blotting, and the integrity of the gradient was verified by monitoring the sedimentation pattern of control EGFP mRNA, whereas the distribution of ribosomal RNA on the gel was used as an indirect marker for the polysome distribution as described previously (27,28). Non-polysomal and polysomal fractions were pooled and subsequently examined by mRNA ligation, reverse transcription, PCR, cloning and sequencing as described previously (6).

Protein analysis

For immunoblot analysis, polyclonal antibodies against DHBV surface antigen (6), GFP (Clontech, Heidelberg, Germany) and firefly luciferase (Promega) were used. Immunoblotting was performed using 10–12% SDS–PAGE as described previously (6). Equal amounts of protein were loaded.

Luciferase assays were performed using the Dual luciferase kit according to the manufacturer's instructions (Promega). The firefly/Renilla ratio was determined and values are given in percentage of the luciferase ratio obtained from positive controls within the same experiment as mean values ± SEM from n observations. For statistical analyses, the independent Student's t-test was used and $P \leqslant 0.05$ was accepted to indicate statistical significance. The cleavage of mRNA and expression of truncated proteins was monitored by simultaneous RNA analysis and immunoblotting.

RESULTS

Stable mRNA cleavage fragments are not observed upon cotransfection of siRNA

We wondered whether the generation of stable RNA cleavage fragments also occurs in the RNAi pathway given the similar cleavage patterns of siRNA/RISC and ASO/RNase H. Pilot experiments revealed that pgRNA and sgRNA expressed from

pGemDHBV were only incompletely cleaved upon cotransfection with siRNAs in LMH cells. This may be explained by stoichiometric reasons or the fact that viral RNA may be partially protected against RISC attack by viral proteins such as the reverse transcriptase and core, both encoded by pgRNA. LMH cells were therefore cotransfected with a construct yielding only sgRNA (pDHBVsg) and ASO DHBV795 or isosequential siRNA794, each directed against a sequence flanking the first start codon (Figure 1A). Viral mRNA was analyzed by northern blots with probes complementary to regions 5′ and 3′ from the cleavage site, respectively, so that the resulting cleavage fragments could be distinguished. Northern-blot analysis revealed that sgRNA was almost abolished and the expression of all preS/S isoforms was equally reduced in the corresponding immunoblots upon cotransfection with siRNA794 (Figure 1B and C). In contrast, a band slightly smaller than sgRNA was detected by northern-blot analysis only with the 3′ probe after cotransfection with ASO DHBV795, whereas no RNA was detected with the 5′ probe consistent with complete cleavage and the generation of stable 3′ mRNA cleavage fragments. Immunoblotting revealed the concomitant expression of p35 and p33 initiated from the second and third initiation codon as described earlier for pGemDHBV [see also Figures 1 and 4 in (6)]. Cotransfection of control siRNA with inverse sequence and single-stranded sense siRNA (ssRNA794) did not influence viral RNA or protein expression, whereas cotransfection of single-stranded antisense siRNA (asRNA794) also caused a decrease in the expression of sgRNA and preS/S protein consistent with previous observations that asRNA is efficiently incorporated into RISC (8).

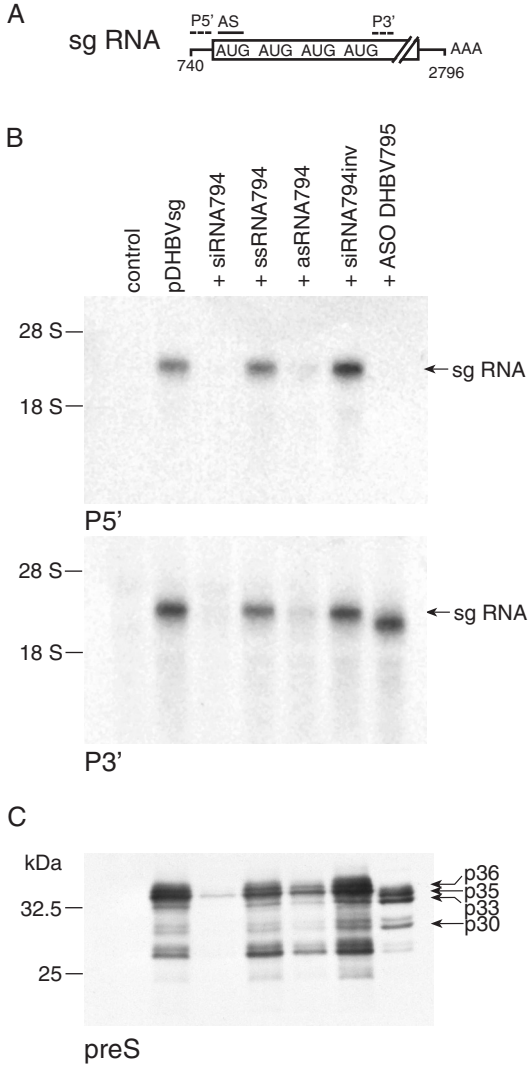

Figure 1. ASO and siRNA differently influence target mRNA stability and translation. (**A**) Schematic diagram of DHBV sgRNA. The initiation codons, hybridization sites for antisense oligos and labeled probes are depicted. The drawing is not to scale. (**B**) Northern-blot analysis with probes discriminating the putative mRNA cleavage fragments upon cotransfection of hepatoma cells with a construct encoding sgRNA and different antisense compounds. Equal amounts of RNA were loaded. (**C**) Immunoblotting of the concomitantly expressed preS/S proteins, different isoforms are indicated. Equal amounts of protein were loaded.

To test whether these differential effects of siRNA794 and ASO DHBV795 on sgRNA were concentration-dependent, LMH cells were cotransfected with various amounts of antisense compounds and northern-blot analysis was performed (Supplementary Figure S1). Small amounts of uncleaved sgRNA were still detected by both probes with all concentrations of siRNA794. In contrast, one-third of sgRNA was still detected by the 5′ probe (i.e. uncleaved) with the lowest concentration of ASO DHBV795 but diminished to background levels with higher concentrations. In contrast, 3′ cleavage fragments were detected with increasing concentrations of ASO DHBV795 in approximately the same amount as uncleaved sgRNA. It should be noted that the transfection efficiency was reduced with increasing ASO amounts as judged from the EGFP signal.

The activity of siRNA/RISC is rather localized in the cytoplasm and intermediate mRNA cleavage fragments generated by siRNA/RISC might therefore be readily degraded by the cytoplasmic RNA decay machinery. Stable 3′ mRNA cleavage fragments generated by ASO/RNase H have been previously shown to lack a 5′ cap structure, an important enhancer of nucleocytoplasmic transport (29). If ASO/RNase H-mediated cleavage occurred predominantly in the nucleus, uncapped 3′ mRNA cleavage fragments might accumulate within the protected nuclear compartment and thus escape from the cytoplasmic mRNA decay machinery. To address this possibility, we analyzed total cellular and cytoplasmic RNA prepared from the same cells cotransfected with pDHBVsg and ASO by northern blotting. The distribution of total and cytoplasmic sgRNA was not affected by cotransfection of either ASO DHBV795 or DHBV795miss (Figure 2). The amount of each RNA was quantified and revealed that ~50% of sgRNA was cytoplasmic independent of the ASO used. The percentage of EGFP mRNA in the cytoplasm was higher amounting to ~70%. The appearance of stable 3′ mRNA fragments upon ASO/RNase H-mediated cleavage is therefore not due to nuclear accumulation.

Oligonucleotides with a modification in the 2′ position such as 2′-*O*-methyl are RNase H-incompetent and can therefore be used as a negative control to demonstrate the involvement of RNase H in antisense experiments (4,30). In contrast to the effects observed after cotransfection of ASO DHBV795, the expression of viral mRNA and surface proteins was not influenced by cotransfection of pGemDHBV and isosequential

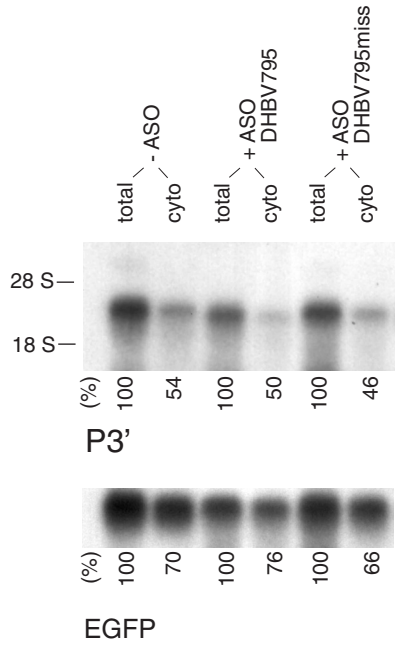

Figure 2. The amount of cytoplasmic sgRNA is not influenced by ASO/RNase H-mediated cleavage. Northern-blot analysis of total cellular and cytoplasmic RNA isolated from the same sample of cells upon cotransfection of pDHBVsg with the indicated ASO. Probes complementary to a portion of sgRNA located 3′ to the putative cleavage site or to EGFP were used, respectively. EGFP was cotransfected as internal control. Equal amounts of RNA were loaded. The amount of cytoplasmic RNA in comparison with total RNA is given in percent. Representative experiment, ($n = 3$).

2′-*O*-methyl-modified oligonucleotides, thus providing indirect evidence that RNase H is involved in the generation of stable 3′ mRNA cleavage fragments (data not shown).

Association of stable 3′ mRNA cleavage fragments with polysomes

We next aimed at establishing a more direct link between cytoplasmic mRNA cleavage fragments and the translation apparatus by polysome analysis using sucrose gradient centrifugation. Expression plasmids encoding both pgRNA and sgRNA were used in these experiments (Figure 3A). Pilot experiments revealed that the sedimentation patterns of RNA-containing core particles and polysomes overlap (data not shown). Hepatoma cells were therefore cotransfected with a DHBV core deletion mutant (pHTD-Dcore$^-$), different ASO and EGFP as internal control. However, cotransfection of ASO DHBV795 with pHTD-D core$^-$ or wild-type pGemDHBV was shown to result in a similar distribution of stable 3′ mRNA cleavage fragments over the gradient because the core was not expressed after endonucleolytic cleavage of pgRNA (data not shown). Sucrose gradient centrifugation of cytoplasmic extracts was performed and fractions were analyzed by northern blotting. The absorbance profile indicated that polysomes were present throughout fractions 7–10 (Figure 3B). The profile and the polysomal association of control EGFP mRNA were not affected by the different ASO used. Northern-blot analysis revealed two major bands of viral RNA corresponding to pgRNA and sgRNA with pgRNA being more abundantly expressed. Uncleaved sgRNA was predominantly found in polysomal fractions 9 and 10, whereas pgRNA was evenly distributed throughout the gradient, consistent with a moderate translational efficiency. This was expected for the core-deficient pgRNA transcribed from pHTD-Dcore$^-$ because core is a major gene product of pgRNA. pgRNA was no longer detectable after cotransfection of ASO DHBV795 consistent with complete mRNA cleavage. The signal co-migrating with 5S RNA in the supernatant is most likely due to unspecific labeling of small RNA and degradation products. Stable 3′ mRNA cleavage fragments predominantly co-sedimented with non-polysomal fractions 2–5; however, a significant amount of mRNA still co-sedimented with polysomal fractions 7–10. These findings indicate that the stable 3′ mRNA cleavage fragments serve as a template for translation. But the mRNA distribution was consistent with a reduced translational efficiency compared to uncleaved sgRNA or mRNA coding for EGFP. To test whether the mRNA sedimentation properties were determined by the binding of polysomes, the sedimentation profiles were also examined by sucrose gradient centrifugation after $MgCl_2$ was replaced by EDTA. This causes the dissociation of ribosomes from mRNA, whereas most non-ribosomal RNA–protein complexes are not disrupted (26). In the presence of EDTA, viral and EGFP mRNA co-sedimented predominantly with fractions 2–4 indicating that the sedimentation profile was indeed due to polysomal association (Supplementary Figure 2). Careful analysis of the gradients revealed that non-polysomal pgRNA migrated further into the gradient than non-polysomal sgRNA or EGFP mRNA. This difference was still detected after the dissociation of ribosomes in the presence of EDTA and may be determined by the size of the respective RNAs. In conclusion, these data provide direct evidence that cytoplasmic 3′ mRNA cleavage fragments serve as a template for translation in hepatoma cells even if the polysomal distribution was consistent with reduced translational efficiency.

Translation of stable 3′ mRNA cleavage fragments is, at least in part, cap-independent but 5′ end-dependent

Stable 3′ mRNA cleavage fragments isolated from total cellular extracts were shown previously to be uncapped by RNA ligation and subsequent RT–PCR (6). Therefore, it was questioned whether translation of these fragments involves a cap-independent mechanism or whether recapping occurs. If recapping was essentially required for the translation of stable 3′ mRNA cleavage fragments, no uncapped fragments should be detected in the polysome-associated RNA. To address this question, LMH cells were cotransfected with pGemDHBV and ASO DHBV795 followed by sucrose gradient centrifugation of cytoplasmic extracts. After fractionation, the gradient was directly analyzed by northern blotting without prior determination of the absorbance in order to minimize mRNA degradation before ligation and RT–PCR. The integrity of the gradient was instead verified by monitoring the sedimentation pattern of EGFP mRNA as internal control and the ribosomal RNA as described previously (27,28). Polysomal fractions 12–18 (corresponding to fractions 7–10 in Figure 3B) and non-polysomal fractions 4–10 (corresponding to fractions 2–5 in Figure 3B) were pooled and subsequently analyzed

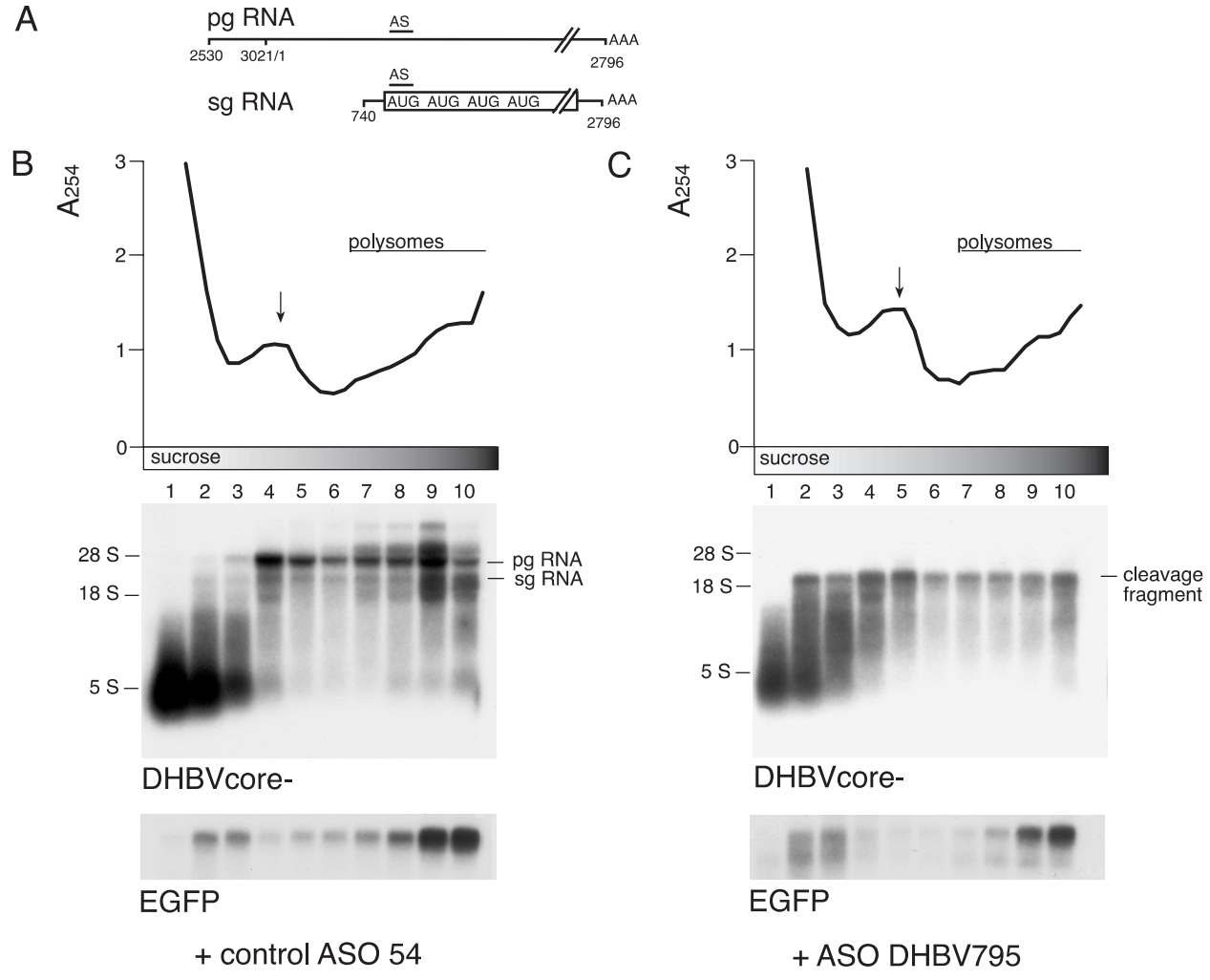

Figure 3. Stable 3′ mRNA cleavage fragments are associated with polysomes. (**A**) Schematic diagram of the major transcripts of DHBV. The drawing is not to scale. (**B**) Polysome analysis of mRNA after cotransfection with control ASO 54 (B) or ASO DHBV795 (**C**) by sucrose gradient centrifugation. Cytoplasmic extracts were separated on a 10–50% sucrose gradient and fractionated. After fractionation, the absorbance at 254 nm was determined for each of the 30 fractions and is shown at the top of each panel. The position of non-polysomal ribosomal subunits (arrows) and of polysomes is indicated. Fractions from the bottom of the gradient are shown on the right. Three fractions each were pooled and equal volumes of each fraction were loaded for northern-blot analysis using labeled DHBV and EGFP DNA fragments as a probe, respectively. The positions of pgRNA, sgRNA and 3′ cleavage fragments are indicated. The polysomal distribution of EGFP RNA was used as internal control.

by RNA ligation and RT–PCR as described previously (6). In this assay, ligation and subsequent amplification of an ∼0.4 kb PCR product comprising the poly(A) tail, cleavage site and adjacent sequences only occurs if the mRNA 5′ terminus is phosphorylated (i.e. uncapped, Figure 4A). It should be noted that only DHBV RNA ligated to its own 3′ terminus or to another DHBV RNA is amplified in this protocol. It is therefore likely that only a very small subset of uncapped 3′ mRNA cleavage fragments is detected with this assay given the vast amount of unrelated mRNA 3′ termini present in the cell. However, PCR products with the predicted size could indeed be amplified from the polysomal and non-polysomal pools indicating that these pools include uncapped 3′ mRNA cleavage fragments (Figure 4B). It should be noted that two further PCR products were generated by internal binding of the primers on pgRNA and residual viral DNA. Their amplification was comparatively efficient because it did not necessitate ligation of the mRNA, the rate-limiting step of this protocol (6). These findings suggest that a cap-independent mode of translation qualitatively contributes to the generation of truncated proteins from stable 3′ mRNA cleavage fragments. However, as it cannot be ruled out that the cleavage fragments are recapped in parallel thus supporting a cap-dependent mode of translation, the impact of cap-independent translation cannot be assessed more quantitatively with this assay.

The ∼0.4 kb PCR fragments were analyzed further by cloning and sequencing. The cleavage sites determined in 12 clones were located in the 3′ region of the ASO/mRNA heteroduplex consistent with endonucleolytic cleavage by RNase H (Figure 4C). In parallel, expression of p35 and p33 was observed by immunoblotting of the cytoplasmic extracts (data not shown). Sequencing of the clones obtained from the polysomal pool revealed that the distance between the 5′ terminus and the next start codon yielding p35 was very short comprising only 7–20 nt. This short distance suggests that the translation of 3′ mRNA cleavage fragments involves 5′ end-dependent binding of ribosomes.

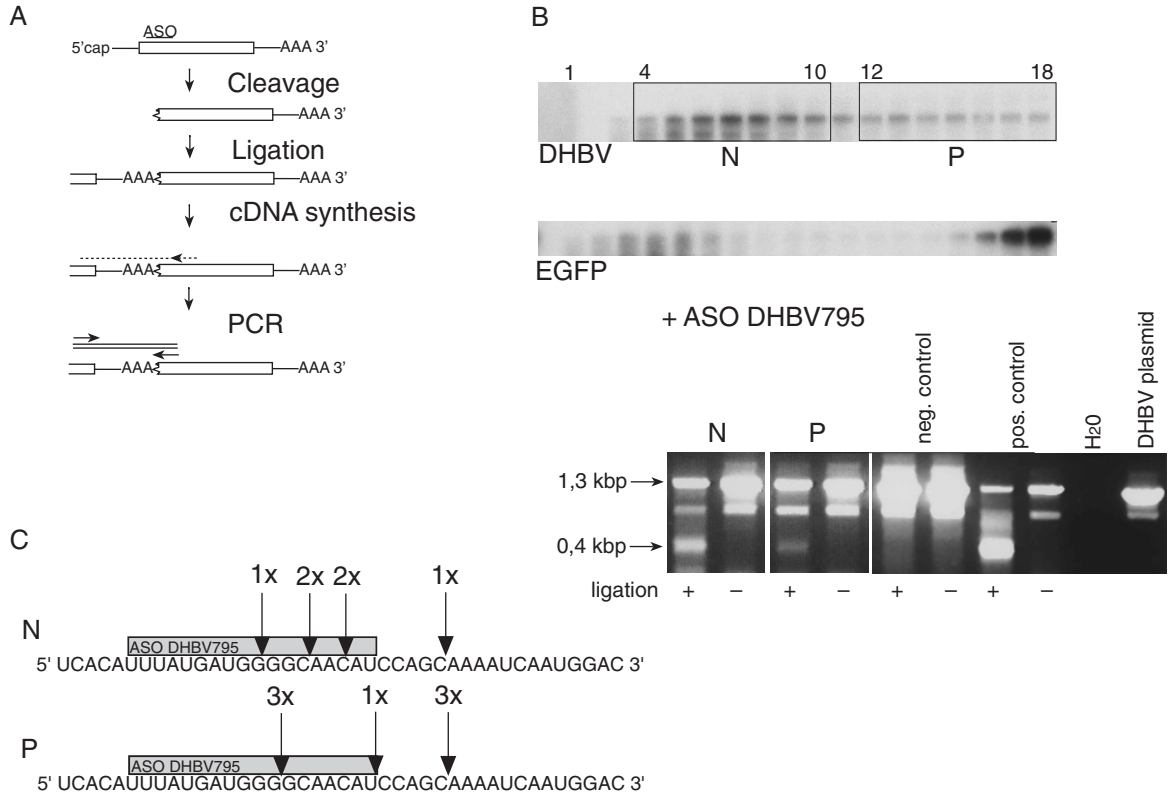

Figure 4. The polysomal pool of RNA contains uncapped 3′ mRNA cleavage fragments. (**A**) Strategy to examine the mRNA 5′ capping status by RNA ligation and subsequent RT–PCR. See Results for details. (**B**) Northern-blot analysis of RNA from cells cotransfected with DHBV and ASO DHBV795 followed by polysome analysis (top). Non-polysomal (N) and polysomal fractions (P) were pooled and the capping status of stable 3′ mRNA cleavage fragments was examined. Agarose gel photograph of the PCR products (bottom). Ligation and subsequent amplification of ~0.4 kb PCR product indicated that the sample contained uncapped 3′ mRNA cleavage fragments. It should be noted that the two larger products were amplified from pgRNA and DHBV DNA due to internal binding of the primers. Amplification of these longer products did not reflect the capping status as it was independent of the ligation step. Total cellular RNA from DHBV-transfected cells without (negative control) and with ASO DHBV795 (positive control) was used as controls. (**C**) Six clones from the non-polysomal and polysomal pool each were cloned and sequenced. The position of the 5′ terminus of stable 3′ mRNA cleavage fragments corresponding to the RNase H cleavage site is indicated.

Stable 3′ mRNA cleavage fragments are translated with moderate efficiency

Translational efficiency will be critical to determine the functional relevance of uncapped 3′ mRNA cleavage fragments. We therefore sought a more quantitative assay to determine the translational efficiency using a construct consisting of the sgRNA 5′-UTR and preS portion fused in frame to firefly luciferase (preS-Luc; Figure 5A). We anticipated that the yield of luciferase fusion proteins should be a good indirect marker for translational efficiency. LMH cells were cotransfected with preS-Luc, a *Renilla* luciferase construct as internal control and different ASO, and subsequently analyzed by northern-blot analysis and immunoblotting. Luciferase activity was normalized to the cotransfected *Renilla* control to account for differences in transfection efficiency or unspecific effects of the respective ASO on gene expression.

Cotransfection of preS-Luc with each ASO resulted in the generation of distinct stable 3′ mRNA cleavage fragments, and faint bands consistent with 5′ cleavage fragments were detected by the 5′ probe (Figure 5B). Interestingly, the amount of 3′ cleavage fragments was increased 3-fold upon cotransfection with ASO DHBV795 and 2-fold after cotransfection with ASO DHBV874, but remained unchanged upon cotransfection with ASO Luc. This was paralleled by increased expression of *Renilla* luciferase. We therefore hypothesize that cotransfection of the respective ASO may influence the transfection efficiency of the luciferase plasmids. However, this effect was accounted for by the normalization of firefly to *Renilla* luciferase activity. Truncated preS luciferase fusion proteins were identified by immunoblotting using antibodies against preS and luciferase (Figure 5C and data not shown). Size analysis and comparison to the expression pattern of preS/S proteins suggested that the synthesis of preS-Luc proteins was predominantly initiated at the first start codon and the fourth start codon. After cotransfection with ASO DHBV795 directed against the first start codon, the predominant bands were consistent with translation from the second start codon and from the fourth start codon. Luciferase activity was significantly reduced to 13.2 ± 1.7% (n = 12) compared to translation from uncleaved mRNA. A single band consistent with a fusion protein initiated from the fourth start codon was detected by immunoblotting after cotransfection with ASO DHBV874 directed against the third start codon. Interestingly, luciferase activity was reduced to a lesser extent than after cotransfection of ASO DHBV795 (24.9 ± 5.5%, n = 6). These findings indicate that stable 3′ mRNA cleavage fragments are translated with moderate efficiency which is influenced by the ASO used.

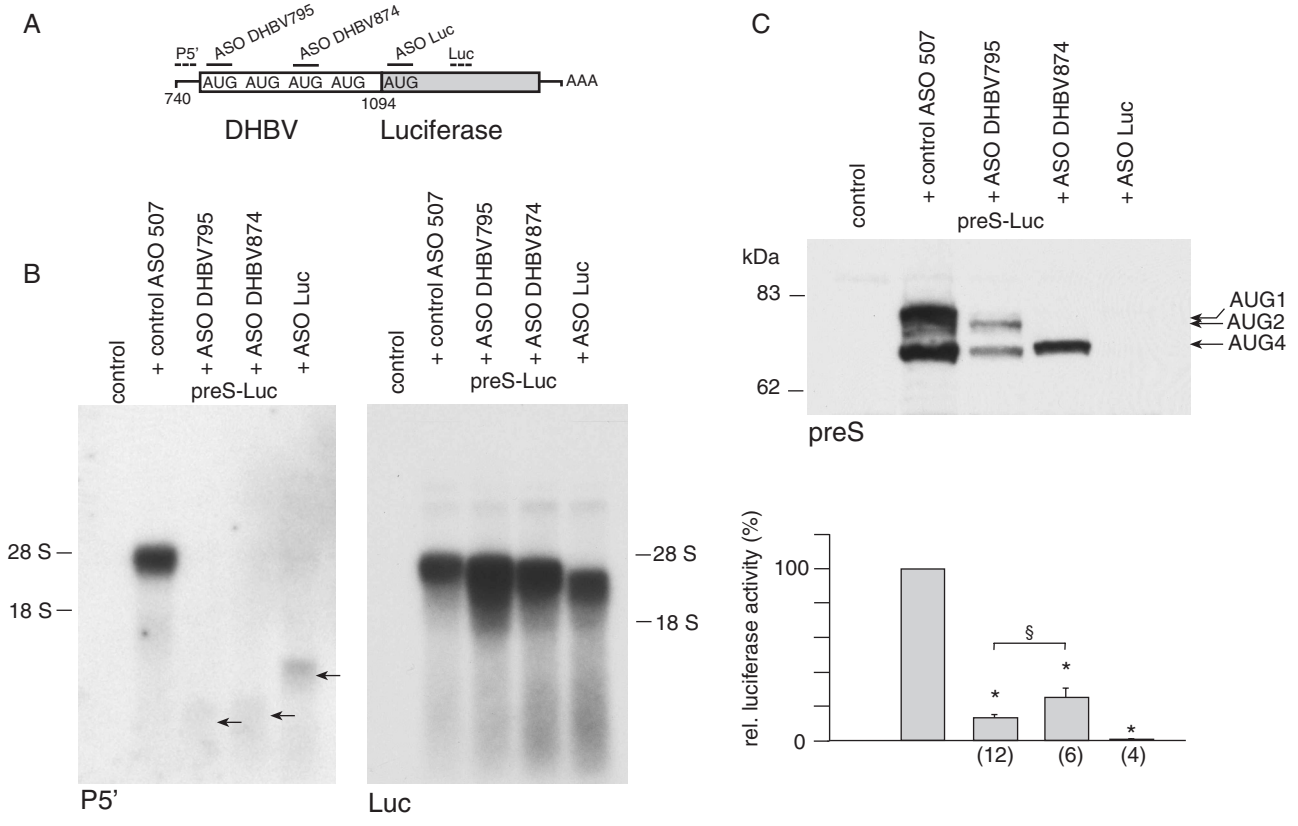

Figure 5. Stable 3′ mRNA cleavage fragments are translated with moderate efficiency. (**A**) Translation of stable 3′ mRNA cleavage fragments was quantified using a preS luciferase fusion construct. The binding sites for different ASO and labeled probes are shown. The drawing is not to scale. (**B**) Northern-blot analysis with probes discriminating RNA cleavage fragments upon cotransfection of preS-Luc with different ASO. Faint bands consistent with 5′ cleavage fragments are indicated by arrows. (**C**) Immunoblotting of luciferase fusion proteins upon cotransfection with different ASO is depicted (top). Equal amounts of protein were loaded. Quantification of protein yield by luciferase activity (bottom). Values are given in percent compared to luciferase activity obtained after cotransfection of control ASO. The number of observations is given in brackets. Asterisks indicate a statistically significant difference compared with control ASO treated cells, whereas, the section mark symbol indicates a statistically significant difference between cells cotransfected with ASO DHBV795 and DHBV874.

Luciferase expression decreased almost to background levels after cotransfection of ASO Luc directed against the luciferase initiation codon (0.6 ± 0.1%, $n = 4$). Interestingly, cotransfection of ASO Luc also resulted in the generation of stable 3′ mRNA cleavage fragments even if no initiation codon with favorable Kozak consensus sequence was available downstream the cleavage site. This finding indicates that translation is unlikely to be required for the stabilization of 3′ mRNA cleavage fragments. Furthermore, stable 3′ mRNA cleavage fragments generated after cotransfection of preS-Luc and ASO DHBV795 were also efficiently ligated and did therefore not differ from DHBV fragments with regard to their capping status (data not shown).

The DHBV preS region does not exhibit IRES activity

To exclude the possibility that IRES activity within the DHBV preS region may account for the translation of uncapped 3′ mRNA cleavage fragments, a dicistronic vector with EGFP as first cistron and preS-Luc as second cistron was designed (Figure 6A). Dicistronic vectors are commonly used to study IRES activity because translation of the downstream cistron does usually not occur in the absence of an IRES (18). The dicistronic construct was cotransfected with control ASO or ASO DHBV795. Monocistronic preS-Luc served as positive control. After cotransfection of control ASO, the 5′ cistron EGFP was readily expressed, whereas no luciferase fusion proteins could be detected indicating that no significant IRES activity was present within the DHBV preS region (luciferase activity 0.8 ± 0.1%, $n = 3$; Figure 6B). After cotransfection of ASO DHBV795, stable 3′ mRNA cleavage fragments with the same size as the fragments obtained after cotransfection of monocistronic preS-Luc mRNA were observed by northern-blot analysis (data not shown). EGFP expression decreased after ASO-mediated cleavage of the bicistronic RNA, whereas luciferase expression was restored to levels obtained after cleavage of monocistronic RNA (monocistronic 13.5 ± 1% versus dicistronic 13.6 ± 0.3%, $n = 3$ each; Figure 6B). Residual EGFP expression after cotransfection with ASO DHBV795 is explained by a small amount of uncleaved dicistronic mRNA. Therefore, IRES activity was not present within the DHBV preS region and did not contribute to the translation of uncapped 3′ mRNA cleavage fragments.

Contribution of the subcellular compartment to the generation of stable 3′ mRNA cleavage fragments

RNase H activity has been observed in the nucleus and in the cytoplasm, respectively (5). A cytoplasmic activity of

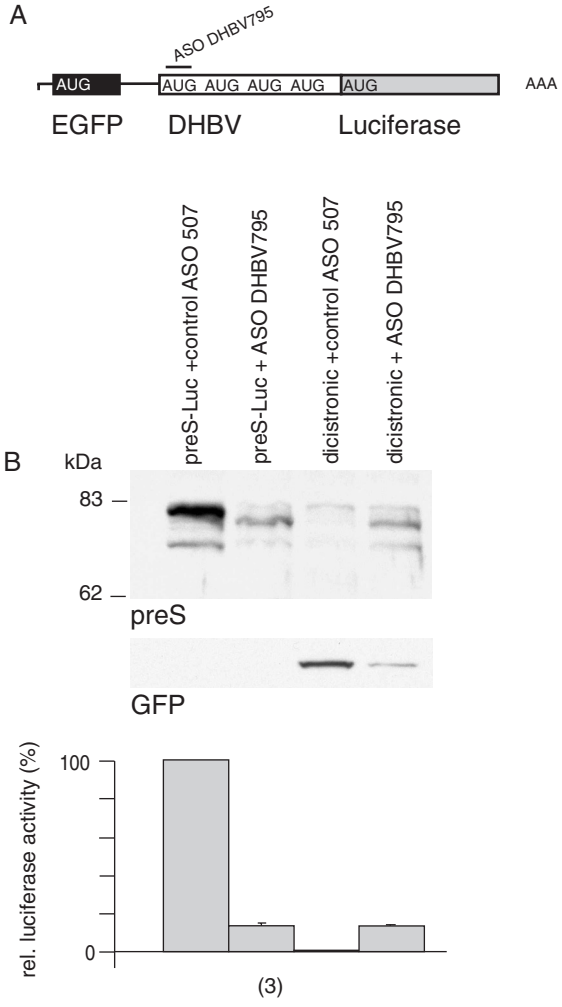

Figure 6. The DHBV preS region does not display IRES activity. (**A**) Schematic diagram of a dicistronic vector comprising EGFP and preS Luc is shown. (**B**) Immunoblotting of preS luciferase fusion proteins and EGFP upon cotransfection with ASO. Monocistronic preS-Luc served as positive control. Equal amounts of protein were loaded. Relative luciferase activity was compared to luciferase activity obtained after cotransfection of the monocistronic construct with control ASO and is given in percent. The number of observations is given in brackets.

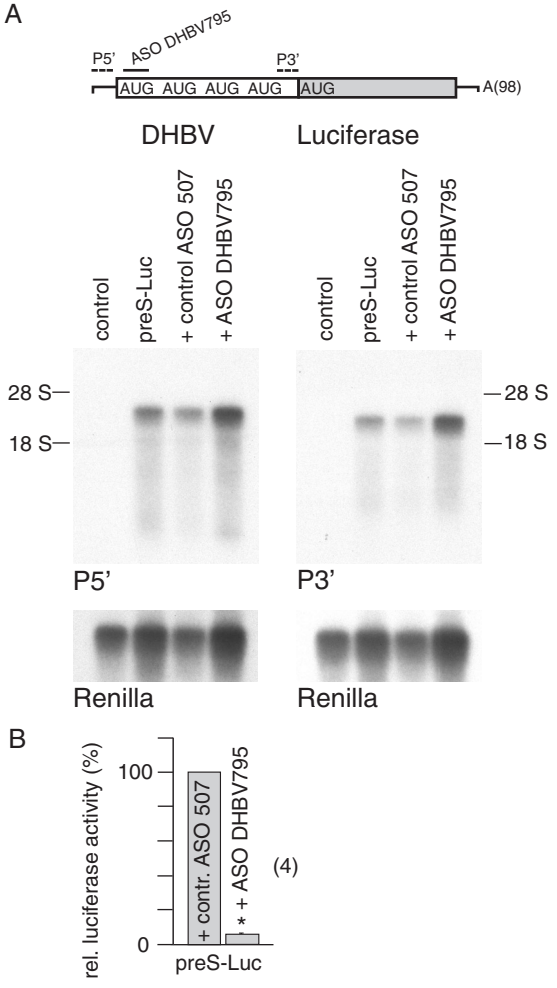

Figure 7. RNase H activity is not observed in the cytoplasm. (**A**) Polyadenylated preS-Luc mRNA was *in vitro* transcribed and capped. The hybridization sites for ASO DHBV795 and labeled probes are depicted. The drawing is not to scale (top). Northern-blot analysis upon cotransfection with ASO DHBV 795 is depicted (bottom). Equal amounts of RNA were loaded. Cotransfected renilla mRNA is shown as control. (**B**) Relative luciferase activity obtained after cotransfection of mRNA and ASO DHBV795. Values are given in percent compared to luciferase activity obtained after cotransfection of control ASO. The number of observations is given in brackets. The asterisk indicates a statistically significant difference.

ASO/RNase H may facilitate the translation of stable 3′ mRNA cleavage fragments because ribosomes could then be recruited by a cap-dependent mechanism before endonucleolytic cleavage. These ribosomes could then cycle on mRNA cleavage fragments and support their translation even if the capped 5′ end was removed by endonucleolytic cleavage. To address this possibility, *in vitro* transcribed, capped and polyadenylated preS-Luc mRNA was cotransfected with ASO DHBV795 and *Renilla* mRNA as internal control. We assumed that transfected *in vitro* transcribed mRNA should be localized within the cytoplasm and that the effects observed after cotransfection should therefore reflect a cytoplasmic event. Cells were harvested 4 h after transfection and analyzed. Surprisingly, mRNA was quantitatively not influenced by ASO DHBV795 and no cleavage fragments were observed (Figure 7A). In contrast, the expression of luciferase fusion proteins was significantly reduced to 5.5 ± 0.3% ($n = 4$) after cotransfection of ASO DHBV795 compared with the cotransfection of control ASO (Figure 7B). These findings suggest that the decline in luciferase activity was rather due to sterical inhibition of translation than to cytoplasmic activity of RNase H. In keeping with this notion, immunoblotting revealed that expression of all preS-Luc isoforms was equally reduced and no shift of translation towards smaller isoforms was observed (data not shown). The absence of cytoplasmic RNase H activity indicates that the translation of stable 3′ mRNA cleavage fragments is unlikely to involve cap-dependent initiation of translation prior to cytoplasmic cleavage.

DISCUSSION

Our observation of stable 3′ mRNA cleavage fragments may severely counteract ASO/RNase H-based applications by

the expression of truncated proteins. To address the question whether the generation of stable 3′ mRNA cleavage fragments is restricted to the ASO/RNase H pathway, we compared the effects of isosequential ASO and siRNA directed against hepadnaviral sequences because similar cleavage patterns have been reported for RNase H and RISC (8,9). Furthermore, RISC-induced cleavage fragments have been observed in cytoplasmic extracts from human and *Drosophila* cells (8,31). In contrast, we could not observe any stable mRNA fragments and translation of truncated proteins after the cotransfection of siRNA directed against hepadnaviral sequences in hepatoma cells. In addition to previous studies comparing the action of siRNA and ASO quantitatively (32,33), our results suggest that siRNA may be safer than ASO with respect to potential side effects resulting from the generation of stable mRNA cleavage fragments and their translation. It is not known how the mRNA fragments resulting from siRNA/RISC-mediated cleavage are further degraded, but an additional RISC-associated exonucleolytic activity may be involved in this process (34).

Size analysis of the cleavage fragments, determination of the cleavage sites by RNA ligation and the observation that cleavage could not be induced by RNase H-incompetent oligonucleotides all suggest that RNase H is involved in the generation of stable 3′ mRNA cleavage fragments. At least two different isoforms of cellular RNase H have been characterized, but direct evidence for their involvement in the ASO pathway is still limited (5,9,35). RNase H activity has also been isolated from various viruses including DHBV (36). However, hepadnaviral RNase H was unlikely to contribute to our findings because stable 3′ mRNA cleavage fragments were also observed after cotransfection of constructs without viral RNase H activity, such as pDHBVsg or preS-Luc. We therefore conclude that the generation of stable 3′ mRNA cleavage fragments is restricted to endonucleolytic cleavage induced by ASO and cellular RNase H.

We furthermore provide direct evidence that mRNA cleavage fragments assemble with polysomes and serve as a template for translation. Analysis of polysome-associated cleavage fragments also revealed insights into the mechanisms contributing to their translation. The 5′ cap structure is considered to play an essential role in promoting initiation of translation *in vitro* and *in vivo* (16,17,37). RNA ligation and subsequent RT–PCR was used here to confirm that uncapped mRNA cleavage fragments are associated with polysomes, suggesting that a cap-independent mechanism qualitatively contributes to the translation of stable 3′ mRNA cleavage fragments. However, it cannot be ruled out that the cleavage fragments are recapped in parallel thus supporting a cap-dependent mode of translation and the impact of cap-independent translation cannot be assessed more quantitatively with this assay. Capping is a very early event of mRNA transcription occurring after ~20–30 nt have been synthesized and necessitates close interactions between the capping enzymes and RNA polymerase II (29,38). To our knowledge, a reaction that adds a 5′ cap structure to an otherwise mature mRNA has not been described so far, raising the question whether recapping of stable 3′ mRNA cleavage fragments occurs in the cell.

Several mechanisms may account for the translation of uncapped mRNA including 5′ end-dependent or internal binding of ribosomes (39). Only few studies have examined cap-independent translation in the absence of an IRES structure *in vivo*. It was shown that 5′ end-dependent binding of ribosomes with subsequent ribosomal scanning was involved in the translation of uncapped RNA generated by polymerase III (40,41). More insights regarding the initiation factors that mediate ribosomal binding to the 5′ terminus stem from experiments with translation extracts, where it has been shown *in vitro* that the central domain of eIF4G may be involved, and that translation of uncapped mRNA was even enhanced upon proteolytic cleavage of eIF4G (15,42). In addition, structures within the 3′-UTR such as the poly(A) tail or viral sequences have also been shown to mediate the recruitment of ribosomes to the mRNA (16,43). However, most examples of cap-independent translation in viral and cellular mRNAs have been reported to involve IRES-mediated initiation.

Our data suggest that stable 3′ mRNA cleavage fragments are translated by a 5′ end-dependent mechanism and subsequent ribosomal scanning for the following reasons. Sequencing of polysome-associated and uncapped stable 3′ mRNA cleavage fragments revealed that the initiation codon giving rise to the preS/S p35 isoform and the 5′ terminus are separated by only 7–20 nt. This short distance should be sufficient for the attachment of ribosomes to the 5′ end because translation of an uncapped mRNA with a distance of only 8 nt between the 5′ terminus and initiation codon has earlier been reported (44). However, the first start codon available on stable 3′ mRNA cleavage fragments yielding p35 has a suboptimal consensus sequence and a position very close to the 5′ terminus. The well-established scanning mechanism predicts that this initiation codon will be bypassed by some of the ribosomes (14). These ribosomes will reach the next start codon downstream yielding p33. Smaller preS/S protein isoforms were almost not expressed indicating that spurious 5′ end-independent internal initiation does not occur. In keeping with this notion, no IRES activity was observed within the DHBV preS region using a dicistronic construct. Internal initiation was therefore, unlikely to contribute to the translation of stable 3′ mRNA cleavage fragments.

RNase H activity has been observed in the nucleus and in the cytoplasm, respectively (5). If RNase H-mediated cleavage occurred predominantly in the cytoplasm, ribosomes could also be recruited before endonucleolytic cleavage by a cap-dependent mechanism. These ribosomes could cycle on the mRNA even after the capped 5′ terminus had been removed by ASO/RNase H. This hypothesis is supported by the observation that interaction between the 5′ cap and eIF4E is essential for the recruitment of ribosomes, but dispensable for each round of translation once the ribosome cycles on the mRNA (45). However, cap-dependent initiation before endonucleolytic cleavage is unlikely to contribute to the translation of stable 3′ mRNA cleavage fragments, as we did not observe any RNase H activity in the cytoplasm upon cotransfection of *in vitro* transcribed mRNA and ASO. RNA transfections have been used earlier to demonstrate that a nuclear event was required for proper IRES function on cellular RNA (46,47). We therefore propose that a nuclear mode of action of ASO/RNase H is involved in the generation of stable 3′ mRNA cleavage fragments. The nuclear localization of RNase H activity is also consistent with previous reports demonstrating that ASO also attack pre-mRNA before splicing and that

nuclear accumulation of ASO coincides with the inhibition of gene expression (32,48,49).

It was unexpected in the light of this finding that the amount of cytoplasmic RNA was not influenced by ASO/RNase H-mediated cleavage, as the 5′ cap structure is considered an important enhancer of nuclear export. Such transport may be facilitated by the fact that most hepadnaviral mRNAs are unspliced (50), as ASO-mediated cleavage before splicing has been shown to result in the nuclear accumulation of the RNA (48). Cytoplasmic transport is further enhanced by a RNA element in HBV (51), but similar structures have, to our knowledge, not been described in DHBV. However, the exact mechanisms supporting the nuclear export of uncapped 3′ mRNA cleavage fragments remain to be elucidated.

The translational efficiency of stable 3′ mRNA cleavage fragments will be critical to determine the impact of our findings for future antisense applications. Polysome analysis and expression of firefly fusion proteins indicate a moderate translational efficiency amounting to 13–24% compared with translation of uncleaved mRNA, depending on the ASO used. However, protein analysis (Figures 1C and 5C) suggests that the efficiency of translation may be even higher for preS/S proteins without the luciferase portion and may also be influenced by structures within the target mRNA. The efficiencies reported elsewhere were lower in yeast (4–6%) and in a mammalian cell line (2%) (16,17). However, these efficiencies obtained after transfection of uncapped *in vitro* transcribed mRNA cannot be compared directly to the efficiencies measured here after endonucleolytic cleavage of *in vivo* transcribed mRNA.

In conclusion, we provide evidence that ASO directed against hepadnaviral sequences specifically induce the generation of stable 3′ mRNA cleavage fragments by the action of cellular RNase H. Translation of these fragments likely involves 5′ end-dependent and, at least in part, cap-independent initiation. Even if the efficiency of this process may be moderate, it should be sufficient to result in potential biological effects. As DHBV transcripts are generated by host cellular polymerase II, we assume that the phenomena examined here will also apply to non-viral RNA. Our findings should therefore be taken into account when designing antisense applications to prevent potential side effects by the generation of novel polypeptides with unknown biological properties after ASO/RNase H-mediated cleavage of the target mRNA.

SUPPLEMENTARY MATERIAL

Supplementary Material is available at NAR Online.

ACKNOWLEDGEMENTS

The authors wish to thank H. Will for kindly providing preS-specific antibodies, M. W. Hentze and J. Köck for plasmids and V. Brass for critical reading of the manuscript. The study was supported by a grant (Of14/4-3) from the Deutsche Forschungsgemeinschaft to W.B.O.; P.H. and C.T. were funded by postdoctoral fellowships from the Deutsche Forschungsgemeinschaft and the Fritz-Thyssen-Stiftung, respectively. Funding to pay the Open Access publication charges for this article was provided by the University of Freiburg.

REFERENCES

1. Vitravene Study Group (2002) A randomized controlled clinical trial of intravitreous fomivirsen for treatment of newly diagnosed peripheral cytomegalovirus retinitis in patients with AIDS. *Am. J. Ophthalmol.*, **133**, 552–556.
2. Offensperger,W.B., Offensperger,S., Walter,E., Teubner,K., Igloi,G., Blum,H.E. and Gerok,W. (1993) *In vivo* inhibition of duck hepatitis B virus replication and gene expression by phosphorothioate modified antisense oligodeoxynucleotides. *EMBO J.*, **12**, 1257–1262.
3. Dean,N.M. and Bennett,C.F. (2003) Antisense oligonucleotide-based therapeutics for cancer. *Oncogene*, **22**, 9087–9096.
4. Dias,N. and Stein,C.A. (2002) Antisense oligonucleotides: basic concepts and mechanisms. *Mol. Cancer Ther.*, **1**, 347–355.
5. Wu,H., Lima,W.F., Zang,H., Fan,A., Sun,H. and Crooke,S.T. (2004) Determination of the role of the human RNase H1 in the pharmacology of DNA-like antisense drugs. *J. Biol. Chem.*, **279**, 17181–17189.
6. Thoma,C., Hasselblatt,P., Köck,J., Chang,S.F., Hockenjos,B., Will,H., Hentze,M.W., Blum,H.E., von Weizsäcker,F. and Offensperger,W.B. (2001) Generation of stable mRNA fragments and translation of N-truncated proteins induced by antisense oligodeoxynucleotides. *Mol. Cell*, **8**, 865–872.
7. Dykxhoorn,D.M., Novina,C.D. and Sharp,P.A. (2003) Killing the messenger: short RNAs that silence gene expression. *Nature Rev. Mol. Cell. Biol.*, **4**, 457–467.
8. Martinez,J., Patkaniowska,A., Urlaub,H., Lührmann,R. and Tuschl,T. (2002) Single-stranded antisense siRNAs guide target RNA cleavage in RNAi. *Cell*, **110**, 563–574.
9. Wu,H., Lima,W.F. and Crooke,S.T. (1999) Properties of cloned and expressed human RNase H1. *J. Biol. Chem.*, **274**, 28270–28278.
10. Martinez,J. and Tuschl,T. (2004) RISC is a 5′ phosphomonoester-producing RNA endonuclease. *Genes Dev.*, **18**, 975–980.
11. Song,J.J., Smith,S.K., Hannon,G.J. and Joshua-Tor,L. (2004) Crystal structure of argonaute and its implications for RISC slicer activity. *Science*, **305**, 1434–1437.
12. Hershey,J.W.B. and Merrick,W.C. (2000) The pathway and mechanism of initiation of protein synthesis. In Sonenberg,N., Hershey,J.W.B. and Mathews,M.B. (eds), *Translational Control of Gene Expression*. Cold Spring Harbor Laboratory Press, Cold Spring Harbor, NY, pp. 33–88.
13. Pestova,T.V., Kolupaeva,V.G., Lomakin,I.B., Pilipenko,E.V., Shatsky,I.N., Agol,V.I. and Hellen,C.U.T. (2001) Molecular mechanisms of translational initiation in eukaryotes. *Proc. Natl Acad. Sci. USA*, **98**, 7029–7036.
14. Kozak,M. (2002) Pushing the limits of the scanning mechanism for initiation of translation. *Gene*, **299**, 1–34.
15. de Gregorio,E., Preiss,T. and Hentze,M.W. (1998) Translational activation of uncapped mRNAs by the central part of human eIF4G is 5′ end-dependent. *RNA*, **4**, 828–836.
16. Preiss,T. and Hentze,M.W. (1998) Dual function of the messenger RNA cap structure in poly(A)-tail-promoted translation in yeast. *Nature*, **392**, 516–520.
17. Gallie,D.R. (1991) The cap and poly(A) tail function synergistically to regulate mRNA translational efficiency. *Genes Dev.*, **5**, 2108–2116.
18. Hellen,C.U.T. and Sarnow,P. (2001) Internal ribosome entry sites in eukaryotic mRNA molecules. *Genes Dev.*, **15**, 1593–1612.
19. Ganem,D. and Prince,A.M. (2004) Hepatitis B virus infection–natural history and clinical consequences. *N. Engl. J. Med.*, **350**, 1118–1129.
20. Seeger,C. and Mason,W.S. (2000) Hepatitis B virus biology. *Microbiol. Mol. Biol. Rev.*, **64**, 51–68.
21. Fernholz,D., Wildner,G. and Will,H. (1993) Minor envelope proteins of duck hepatitis B virus are initiated at internal pre-S AUG codons but are not essential for infectivity. *Virology*, **197**, 64–73.
22. Mattes,F., Tong,S., Teubner,K. and Blum,H.E. (1990) Complete nucleotide sequence of a german duck hepatitis B virus. *Nucleic Acids Res.*, **18**, 6140.
23. von Weizsäcker,F., Wieland,S. and Blum,H.E. (1995) Identification of two separable modules in the duck hepatitis B virus core protein. *J. Virol.*, **69**, 2704–2707.
24. Iizuka,N., Najita,L., Franzusoff,A. and Sarnow,P. (1994) Cap-dependent and cap-independent translation by internal initiation of mRNAs in cell extracts prepared from *Saccharomyces cerevisiae*. *Mol. Cell. Biol.*, **14**, 7322–7330.

25. Condreay,L.D., Aldrich,C.E., Coates,L., Mason,W.S. and Wu,T.T. (1990) Efficient duck hepatitis B virus production by an avian liver tumor cell line. *J. Virol*., **64**, 3249–3258.
26. Johannes,G. and Sarnow,P. (1998) Cap-independent polysomal association of natural mRNAs encoding c-myc, BiP, and eIF4G conferred by internal ribosome entry sites. *RNA*, **4**, 1500–1513.
27. Mikulits,W., Pradet-Balade,B., Habermann,B., Beug,H., Garcia-Sanz,J.A. and Müllner,E.W. (2000) Isolation of translationally controlled mRNAs by differential screening. *FASEB J*., **14**, 1641–1652.
28. Baker,B.F., Lot,S.S., Condon,T.P., Cheng-Flournoy,S., Lesnik,E.A., Sasmor,H.M. and Bennett,C.F. (1997) 2′-*O*-(2-Methoxy)ethyl-modified anti-intercellular adhesion molecule 1 (ICAM-1) oligonucleotides selectively increase the ICAM-1 mRNA level and inhibit formation of the ICAM-1 translation initiation complex in human umbilical vein endothelial cells. *J. Biol. Chem*., **272**, 11994–12000.
29. Proudfoot,N.J., Furger,A. and Dye,M.J. (2002) Integrating mRNA processing with transcription. *Cell*, **108**, 501–512.
30. Chiang,M.Y., Chan,H., Zounes,M.A., Freier,S.M., Lima,W.F. and Bennett,C.F. (1991) Antisense oligonucleotides inhibit intercellular adhesion molecule I expression by two distinct mechanisms. *J. Biol. Chem*., **266**, 18162–18171.
31. Elbashir,S.M., Lendeckel,W. and Tuschl,T. (2001) RNA interference is mediated by 21- and 22-nucleotide RNAs. *Genes Dev*., **15**, 188–200.
32. Vickers,T.A., Koo,S., Bennett,C.F., Crooke,S.T., Dean,N.M. and Baker,B.F. (2003) Efficient reduction of target RNA's by siRNA and RNase H dependent antisense agents: a comparative analysis. *J. Biol. Chem*., **278**, 7108–7118.
33. Grünweller,A., Wyszko,E., Bieber,B., Jahnel,R., Erdmann,V.A. and Kurreck,J. (2003) Comparison of different antisense strategies in mammalian cells using locked nucleic acids, 2′-*O*-methyl RNA, phosphorothioates and small interfering RNA. *Nucleic Acids Res*., **31**, 3185–3193.
34. Caudy,A.A., Ketting,R.F., Hammond,S.M., Denli,A.M., Bathoorn,A.M.P., Tops,B.B.J., Silva,J.M., Myers,M.M., Hannon,G.J. and Plasterk,R.H.A. (2003) A micrococcal nuclease homologue in RNAi effector complexes. *Nature*, **425**, 411–414.
35. ten Asbroek,A.L.M.A., van Groenigen,M. and Baas,F. (2002) The involvement of human ribonucleases H1 and H2 in the variation of response of cells to antisense phosphorothioate oligonucleotides. *Eur. J. Biochem*., **269**, 583–592.
36. Oberhaus,S.M. and Newbold,J.E. (1995) Detection of an RNase H activitiy associated with hepadnaviruses. *J. Virol*., **69**, 5697–5704.
37. Michel,Y.M., Poncet,D., Piron,M., Kean,K.M. and Borman,A.M. (2000) Cap-poly(A) synergy in mammalian cell-free extracts. *J. Biol. Chem*., **275**, 32268–32276.
38. Shatkin,A.J. and Manley,J.L. (2000) The ends of the affair: capping and polyadenylation. *Nature Struct. Biol*., **7**, 838–842.
39. Jackson,R.J. (2000) A comparative view of initiation site selection mechanisms. In Sonenberg,N., Hershey,J.W.B. and Mathews,M.B. (eds), *Translational Control of Gene Expression.* Cold Spring Harbor Laboratory Press, Cold Spring Harbor, NY, pp. 127–183.
40. Gunnery,S. and Mathews,M.B. (1995) Functional mRNA can be generated by RNA polymerase III. *Mol. Cell. Biol*., **15**, 3597–3607.
41. Gunnery,S., Mäivali,Ü. and Mathews,M.B. (1997) Translation of an uncapped mRNA involves scanning. *J. Biol. Chem*., **272**, 21642–21646.
42. Ohlmann,T., Rau,M., Morley,S.J. and Pain,V.M. (1995) Proteolytic cleavage of initiation factor eIF-4γ in the reticulocyte lysate inhibits translation of capped mRNAs but enhances that of uncapped mRNAs. *Nucleic Acids Res*., **23**, 334–340.
43. Wang,S., Browning,K.S. and Miller,W.A. (1997) A viral sequence in the 3′-untranslated region mimics a 5′ cap in facilitating translation of uncapped mRNA. *EMBO J*., **16**, 4107–4116.
44. Pestova,T.V. and Kolupaeva,V.G. (2002) The roles of individual eukaryotic translation initiation factors in ribosomal scanning and initiation codon selection. *Genes Dev*., **16**, 2906–2922.
45. Novoa,I. and Carrasco,L. (1999) Cleavage of eukaryotic translation initiation factor 4G by exogenously added hybrid proteins containing poliovirus $2A^{pro}$ in HeLa cells: effects on gene expression. *Mol. Cell. Biol*., **19**, 2445–2454.
46. Shiroki,K., Ohsawa,C., Sugi,N., Wakiyama,M., Miura,K.I., Watanabe,M., Suzuki,Y. and Sugano,S. (2002) Internal ribosome entry site-mediated translation of Smad5 *in vivo*: requirement for a nuclear event. *Nucleic Acids Res*., **30**, 2851–2861.
47. Stoneley,M., Subkhankulova,T., Le Quesne,J.P.C., Coldwell,M.J., Jopling,C.L., Belsham,G.J. and Willis,A.E. (2000) Analysis of the c-myc IRES: a potential role for cell-type specific *trans*-acting factors and the nuclear compartment. *Nucleic Acids Res*., **28**, 687–694.
48. Condon,T.P. and Bennett,C.F. (1996) Altered mRNA splicing and inhibition of human E-selectin expression by an antisense oligonucleotide in human umbilical vein endothelial cells. *J. Biol. Chem*., **271**, 30398–30403.
49. Marcusson,E.G., Bhat,B., Manoharan,M., Bennett,C.F. and Dean,N.M. (1998) Phosphorothioate oligodeoxyribonucleotides dissociate from cationic lipids before entering the nucleus. *Nucleic Acids Res*., **26**, 2016–2023.
50. Obert,S., Zachmann-Brand,B., Deindl,E., Tucker,W., Bartenschlager,R. and Schaller,H. (1996) A spliced hepadnavirus RNA that is essential for virus replication. *EMBO J*., **15**, 2565–2574.
51. Huang,Z.M. and Yen,T.S.B. (1994) Hepatitis B virus RNA element that facilitates accumulation of surface gene transcripts in the cytoplasm. *J. Virol*., **68**, 3193–3199.